Published in final edited form as:
Cell Metab. 2012 April 4; 15(4): 545–553. doi:10.1016/j.cmet.2012.01.022.

Macrophage Autophagy Plays a Protective Role in Advanced Atherosclerosis

Xianghai Liao[1], **Judith C. Sluimer**[1], **Ying Wang**[1,2], **Manikandan Subramanian**[1], **Kristy Brown**[3], **J. Scott Pattison**[4], **Jeffrey Robbins**[4], **Jennifer Martinez**[5], and **Ira Tabas**[1,2,3,*]

[1]Department of Medicine, Columbia University, New York, NY 10032, USA

[2]Department of Physiology & Cellular Biophysics, Columbia University, New York, NY 10032, USA

[3]Department of Pathology & Cell Biology, Columbia University, New York, NY 10032, USA

[4]Department of Pediatrics, Division of Molecular Cardiovascular Biology, Cincinnati Children's Hospital Medical Center, Cincinnati, OH

[5]Department of Immunology, St. Jude Children's Research Hospital, Memphis, TN 38105

SUMMARY

In advanced atherosclerosis, macrophage apoptosis coupled with defective phagocytic clearance of the apoptotic cells (efferocytosis) promotes plaque necrosis, which precipitates acute atherothrombotic cardiovascular events. Oxidative and endoplasmic reticulum (ER) stress in macrophages are important causes of advanced lesional macrophage apoptosis. We now show that pro-apoptotic oxidative/ER stress inducers trigger another stress reaction in macrophages, autophagy. Inhibition of autophagy by silencing ATG5 or other autophagy mediators enhances apoptosis and NADPH oxidase-mediated oxidative stress, while at the same time rendering the apoptotic cells less well recognized by efferocytes. Most importantly, macrophage ATG5 deficiency in fat-fed *Ldlr*$^{-/-}$ mice increases apoptosis and oxidative stress in advanced lesional macrophages, promotes plaque necrosis, and worsens lesional efferocytosis. These findings reveal a protective process in oxidatively stressed macrophages relevant to plaque necrosis, suggesting a mechanism-based strategy to therapeutically suppress atherosclerosis progression and its clinical sequelae.

INTRODUCTION

In advanced atherosclerosis, death of lesional macrophages, coupled with defective phagocytic clearance of the dead cells ("efferocytosis"), promotes the formation of plaque necrosis (Tabas, 2010). Plaque necrosis is a key distinguishing feature of and likely causative process in the small percentage of atherosclerotic lesions that cause acute atherothrombotic vascular disease, such as myocardial infarction, sudden cardiac death, and stroke (Virmani et al., 2002). *In vivo* data suggest that endoplasmic reticulum (ER) and

*Correspondence: iat1@columbia.edu.

SUPPLEMENTAL INFORMATION

Supplemental Information includes Supplemental Experimental Procedures, Supplemental References, and 4 figures.

oxidative stress play important roles in advanced lesional macrophage death (Lusis, 2000; Moore and Tabas, 2011). When macrophages are exposed to atherosclerosis-relevant factors that trigger these stress reactions, such as oxysterols, oxidized phospholipids (oxPLs), or unesterified "free" cholesterol (FC), ER stress-induced apoptotic pathways are activated (Lusis, 2000; Moore and Tabas, 2011). Moreover, the NOX2 subunit of NADPH oxidase is induced, leading to assembly of active NADPH oxidase complex on lysosomes and pro-apoptotic oxidative stress (Li et al., 2010; Seimon et al., 2010). In response to cell death, efferocytosis is normally rapid and efficient and thereby prevents post-apoptotic necrosis and inflammation (Henson et al., 2001), but for reasons that are not yet known, efferocytosis is defective in advanced atherosclerosis (Schrijvers et al., 2005; Tabas, 2010).

In an attempt to increase our understanding in these areas, we decided to explore the process of autophagy, which can affect both apoptosis and efferocytosis in other settings (Eisenberg-Lerner et al., 2009; Qu et al., 2007). In this regard, we set out to explore how autophagy may effect these processes in advanced atherosclerosis by genetically preventing the autophagic response in macrophages exposed to oxidative/ER stressors *in vitro* and in advanced atherosclerotic lesions *in vivo*. We show that blocking autophagy renders macrophages more susceptible to cell death, worsens the recognition and clearance of the dead cells by efferocytes, and promotes plaque necrosis in a mouse model of advanced atherosclerosis.

RESULTS

Autophagy is induced in macrophages exposed to atherosclerosis-related stimulators of apoptosis

Primary murine macrophages from mice transgenic for a GFP-tagged version of the autophagy effector LC3-II were treated for 6 h with 7-ketocholesterol (7KC), an atherosclerotic lesional oxysterol that promotes oxidative stress, ER stress, and apoptosis in macrophages (Lizard et al., 1998; Myoishi et al., 2007; Li et al., 2010). The 7KC-treated macrophages showed a punctate pattern of fluroscence that is indicative of autophagy induction (Mizushima et al., 2010) (Figure 1A). At the ultrastructural level (Figure 1B), 7KC-treated macrophages had numerous double-membrane structures that were characteristic of autophagosomes. We also explored macrophages incubated with KOdiA-PC, an oxPL typical of those in oxidized LDL, in combination with low-dose thapsigargin, which induces ER stress by inhibiting calcium re-entry into the ER (Seimon et al., 2010). These macrophages also showed the presence of double membrane structures. In contrast, there were very few double membranes in untreated macrophages or in 7KC-treated macrophages from *Atg5*$^{fl/fl}$*Lysmcre*$^{+/-}$ mice, which lack the key autophagy protein ATG5 (Hara et al., 2006). To further document autophagy, we assayed the expression of the LC3-II, which is converted from LC3-I during the early stages of autophagy (Mizushima et al., 2010) (Figure 1C, lanes 1–3, 7–9). When macrophages were incubated with 7KC for 4 h, the expression level of LC3-II was higher than baseline, whereas only the precursor LC3-I was detectable in ATG5-deficient macrophages.

The final stage of autophagy, autophagosome-lysosome fusion, leads to lysosomal degradation of autophagosomal content and proteins, including LC3-II itself. This process of "flux" through lysosomes can be documented by showing a higher level of LC3-II in the presence vs. the absence of the lysosomal inhibitor bafilomycin A1 (Mizushima et al., 2010). We found that 7KC treatment of WT macrophages, but not ATG5-deficient macrophages, increased the difference between the minus- and plus-bafilomycin LC3-II signal, indicative of autophagic flux through lysosomes (Figure 1C, lanes 4–6, 10–12). Similar data were obtained in macrophages incubated with KOdiA-PC/thapsigargin and in macrophages loaded with FC (data not shown). These combined data provide strong

evidence that 7KC and other inducers of macrophage apoptosis relevant to atherosclerosis induce autophagy and promote autophagic flux through lysosomes.

Inhibition of autophagy increases apoptosis in macrophages

To test the role of autophagy in apoptosis, we treated wild-type (WT) and *Atg5*$^{fl/fl}$*Lysmcre*$^{+/-}$ mice with a number of different inducers and found markedly higher cell death in the autophagy-defective macrophages (Figure 2A–B and S1A). Note that Figure 2A includes macrophages treated with thapsigargin plus apolipoprotein(a), an atherogenic protein in humans that induces apoptosis in ER-stressed macrophages through its bound oxPLs (Clarke et al., 2009; Seimon et al., 2010). Apoptosis was also enhanced in a more acute model of autophagy inhibition in which ATG5 or the autophagy effector Beclin1 was silenced using siRNA (Figure 2C).

As shown in Fig. 2B, thapsigargin alone at the dose and time used here showed only a very slight, non-significant trend toward increased apoptosis over baseline, and apoptosis was not significantly increased in ATG5-deficient macrophages. However, tunicamycin, which induces ER stress by inhibiting protein glycosylation, did induce apoptosis, and this was further enhanced by ATG5 deficiency (Figure 2D). In this context, we explored a mouse model in which i.v. tunicamycin induces apoptosis of peritoneal macrophages *in vivo* (Li et al., 2009) and found that apoptosis was ~2-fold higher in *Atg5*$^{fl/fl}$*Lysmcre*$^{+/-}$ vs. control *Lysmcre*$^{+/-}$ mice (Figure 2E).

To test the importance of autophagic flux through lysosomes in the anti-apoptotic effect of autophagy, WT macrophages were treated with 7KC either in the absence or presence of bafilomycin A1 or the combination of pepstatin and E64D, which is another means to inhibit autophagolysosomal degradation. Apoptosis was substantially increased in the presence of the lysosomal inhibitors (Figure 2F), suggesting that the protective effect of autophagy requires the full process of autophagic flux through lysosomes.

Many macrophages in atherosclerotic lesions are “foam cells” filled with cholesteryl ester (CE). Although CE loading *per se* does not cause apoptosis (Feng et al., 2003a), we asked whether it would affect the increase in KOdiA-PC/thapsigargin-induced apoptosis caused by autophagy inhibition (Figure S1B). The data show that in foam cells, as in non-foam cells, ATG5 deficiency enhanced KOdiA-PC/thapsigargin-induced apoptosis. Interestingly, ATG5 deficiency also significantly increased apoptosis in non-treated foam cells, suggesting that CE loading, while not inducing apoptosis by itself, renders the cells more sensitive to the pro-apoptotic effect of autophagy inhibition.

The fact that macrophages exposed to the pro-apoptotic inducers used here eventually die suggests that either the prolonged effect of pro-apoptotic processes overwhelms the protective effect of autophagy or that death occurs because the autophagic response eventually decreases. Indeed, we found that LC3-II flux through lysosomes was lower in macrophages exposed to 7C for 16–18 h vs. 6 h (Figure S1C), and this was not associated with a general defect in lysosomal function (Figure S1D). However, when the late decrease in flux was prevented by treatment with rapamycin at the 12-h timepoint or by adenoviral-mediated transduction with ATG7 (Pattison et al., 2011) (Figure S1E), 7KC-induced apoptosis was not decreased (Figure S1F). These data suggest that the late decrease in autophagolysosomal flux is an effect rather than a trigger of apoptosis and that the protective effect of autophagy is eventually overwhelmed by ongoing pro-apoptotic processes.

Autophagy inhibition increases NADPH oxidase-mediated oxidative stress

NADPH oxidase-mediated oxidative stress is a major mechanism of apoptosis in macrophages exposed to the inducers used in this study (Li et al., 2010; Seimon et al., 2010).

To evaluate its role in autophagy-inhibited macrophages, we first compared WT and ATG5-deficient macrophages for DCF staining, which fluoresceces in the presence of peroxide in a manner parallel to NADPH oxidase activation in ER-stressed macrophages (Li et al., 2010). In all models tested, the percentage of DCF-positive cells was substantially higher in the autophagy-defective group (Figure 2G). Similar data were obtained using a FACS assay for cells stained with CellRox™, which is non-fluorescent in the reduced state but exhibits excitation/emission maxima at 640/665 nm upon oxidation (Figure S2A).

We next used a genetic approach to test the role of NADPH oxidase in the enhancement of apoptosis by autophagy inhibition. The experiment is based on the idea that there are two "components" of apoptosis in autophagy-inhibited macrophages: the "basal" level that occurs in autophagy-competent cells, which is suppressed by NOX2 deficiency (Li et al., 2010), and the additional *increment* above this level that occurs in autophagy-inhibited cells. If this incremental component is also NOX2-dependent, NOX2 deficiency should not only decrease the high level of apoptosis seen in autophagy-inhibited cells to a very low level, but it should also eliminate the difference in apoptosis between autophagy-competent and autophagy-inhibited cells. We therefore compared KOdiA-PC/thapsigargin-induced apoptosis in *Nox2*$^{+/+}$ vs. *Nox2*$^{-/-}$ macrophages treated with scrRNA or *Atg5* siRNA to inhibit autophagy (Figure 2H). The data show that NOX2 deficiency markedly inhibited apoptosis in ATG5-silenced macrophages, and the low level of residual apoptosis was similar to that in autophagy-competent (scrRNA) *Nox2*$^{-/-}$ macrophages. Similar results were obtained using 7KC as the apoptosis inducer (data not shown). In theory, NOX2 deficiency could protect macrophages by increasing autophagy, but this was not the case (Figure S2B). These data are consistent with the hypothesis that autophagy inhibition enhances apoptosis, at least in part, by enhancing NADPH oxidase-induced oxidative stress.

To further explore this hypothesis, we considered two recent findings: (a) NADPH oxidase-induced oxidative stress and apoptosis in macrophages are associated with the assembly of NADPH oxidase complex on lysosomes (Seimon et al., 2010); and (b) autophagy in macrophages can participate in the clearance of phagocytosed bacteria in NADPH oxidase-containing phagolysosomes (Huang et al., 2009), and so NADPH oxidase complex itself may be disrupted in the process as part of homeostatic mechanism to protect the cells against excessive oxidative stress. If so, NADPH oxidase-activated macrophages, such as those occurring in the models explored here, would depend on autophagy to limit the oxidative damage. To test this idea, we used the fluorescence microscopy assay established in the aforementioned study to quantify the association of the NADPH oxidase subunit p47^{phox} with lysosomes (Seimon et al., 2010), with the prediction that autophagy inhibition would disallow the disruption of NADPH oxidase complex and thus increase p47^{phox}-lysosome association. Consistent with our previous data (Seimon et al., 2010), incubation of WT macrophages with KOdiA-PC/thapsigargin, but not either factor alone, increased p47^{phox}-lysosome association (Figure S2C, black bars). As predicted by the hypothesis, p47^{phox}-association was increased by ~55% in ATG5-deficient macrophages (Figure S2C, grey bars), which was not simply due to an increase in *Nox2* induction (Figure S2D). Importantly, inhibition of autophagolysosomal flux with bafilomycin in WT macrophages was able to mimic the effect of ATG5 deficiency, and p47^{phox}-lysosome association was not further increased in this setting by ATG5 deficiency. Similar results were obtained with 7KC (data not shown). In summary, the combined data in this section and in previous studies (Li et al., 2010; Seimon et al., 2010; Huang et al., 2009) support the idea that increased apoptosis in autophagy-inhibited cells involves increased NADPH oxidase-induced oxidative stress, possibly through a process that increases lysosome-associated p47^{phox}.

Defective macrophage autophagy promotes plaque necrosis, macrophage apoptosis, oxidative stress in advanced atherosclerosis

In preparation for the atherosclerosis project using *Atg5*$^{fl/fl}$*Lysmcre*$^{+/-}$*Ldlr*$^{-/-}$ mice, we first showed that the aortic root lesions of Western diet (WD)-fed GFP-LC3-*Ldlr*$^{-/-}$ mice contain cells in macrophage-rich regions that express ATG5 and have macrophages that display a punctate pattern of GFP-LC3 fluorescence typical of autophagy (Figure 3A). We then looked for another autophagy protein, p62/SQSTM1, which is known to accumulate when autophagy flux through lysosomes is defective, *i.e.*, through decreased p62 lysosomal degradation (Bjorkoy et al., 2009) (Figure 3B). p62 immunofluorescence was present in ~10–15% of intimal cells in macrophage-rich areas of lesions of 8-wk WD-fed *Ldlr*$^{-/-}$ mice, and this value increased as lesions progressed in 12-wk and 16-wk WD-fed mice. Interestingly, p62 staining was observed in a few of the acellular necrotic areas in 16-wk lesions, which likely reflects the residual debris from macrophages that had accumulated p62 before they died (Ball et al., 1995; Feng et al., 2003b). Note that the mRNA for *Sqstm1* did not increase between 8 and 16 weeks of WD, indicating that the increase in p62 was not due to transcriptional induction (Figure 3B, right graph). These data further substantiate the presence of autophagy in atherosclerotic lesions and are consistent with the concept that autophagic flux through lysosomes decreases as plaques progress.

To test the functional role of macrophage autophagy in advanced atherosclerosis, we studied 12-wk and 16-wk WD-fed *Lysmcre*$^{+/-}$*Ldlr*$^{-/-}$ (control) and *Atg5*$^{fl/fl}$*Lysmcre*$^{+/-}$*Ldlr*$^{-/-}$ mice. Despite no difference in body weight, plasma lipids and lipoproteins, and plasma insulin between the two groups of mice (Figure S3A–B), lesion and necrotic area in the aortic root were higher in *Atg5*$^{fl/fl}$*Lysmcre*$^{+/-}$*Ldlr*$^{-/-}$ vs. control mice at both time points (Figure 3C–D and S3C). The increase in lesion size appeared to be due to the increase in necrotic areas, because the numbers of lesional macrophages and smooth muscle cells were not increased in the experimental cohort (data not shown). This finding is consistent with the mechanistic hypothesis described herein as opposed to an alternative possibility in which a different process, such as macrophage influx or SMC proliferation, might be increased by autophagy inhibition.

Consistent with the mechanistic data in Figures 2–3, quantitative analysis revealed that macrophage-rich regions of the *Atg5*$^{fl/fl}$*Lysmcre*$^{+/-}$*Ldlr*$^{-/-}$ plaques had more cells positive for TUNEL, activated caspase-3, DHE, and p47 than similar regions in control *Lysmcre*$^{+/-}$*Ldlr*$^{-/-}$ plaques (Figure 4A–B and S4A–B). The increase in apoptosis in the experimental group was not associated with an increase in lesion *Chop* expression (Figure S4C), which is consistent with the macrophage data in Fig. 1C.

Defective autophagy in apoptotic macrophages decreases their phagocytic clearance *in vitro* and in atherosclerosis

The increase in plaque necrosis in the ATG5-deficient mice raised the possibility that the macrophages in these mice had a defect in efferocytosis (Henson et al., 2001; Tabas, 2010). We therefore conducted an in-situ efferocytosis assay, which quantifies the ratio of TUNEL-labeled apoptotic cells in lesions that are associated with F4/80-labeled macrophages vs. unassociated (“free”) (Thorp et al., 2008). The data show a marked decrease in the associated:free ratio in the lesions of the mutant mice, indicative of defective efferocytosis (Figure 4C). To examine this point in a more controlled *in vitro* setting, we first compared the ability of ATF5-deficient vs. control macrophages to engulf apoptotic cells and found equal competency (data not shown). We therefore tested whether apoptotic cells that die with defective autophagy are poorly engulfed by efferocytes. To this end, WT or ATG5-deficient macrophages, or WT macrophages treated with bafilomycin A1, were rendered apoptotic by incubation with 7KC and then labeled with Alexa-595-annexin V (red). Equal

numbers of labeled apoptotic cells were added to Calcein-AM (green)-labeled WT macrophages as a source of efferocytes. The data show that there was less efferocytosis of apoptotic cells that were either ATG5-deficient or had inhibited autophagolysosomal flux (bafilomycin) (Figure 4D). The defect appeared to be in apoptotic cell-efferocyte binding, because the inhibitory effect of apoptotic cell ATG5 deficiency on efferocytosis was recapitulated in a 4°C binding assay (Figure 4E). We also found that when the late decrease in autophagic flux in WT cells undergoing apoptosis was bolstered by rapamycin or adeno-Atg7 (see Figs. S1C), their efferocytosis was increased (Figure S4D). Thus, autophagic flux through lysosomes in macrophages undergoing apoptosis enhances their recognition by phagocytes, and this process can be enhanced further by bolstering autophagy.

DISCUSSION

The data in this study focus on functional relationships between autophagy and two critical cell biological processes in atherosclerotic plaque necrosis, Mφ apoptosis and defective efferocytosis. We found that when autophagy was inhibited *in vitro* and *in vivo*, apoptosis was increased and recognition of the autophagy-inhibited dead cells by efferocytic phagocytes was decreased. We infer from these data that autophagy can induce two independent protective actions, which in normal physiology may function to delay cell death in case repair is possible but also ensure that the cells are efficiently cleared by neighboring phagocytes if repair is not possible.

The findings herein raise a number of interesting mechanistic questions for future study. First, the type of autophagy that is involved in protection from apoptosis and oxidative stress and in mediating efficient efferocytosis needs to be defined. The finding of double membranes in a our cell culture model indicates that autophagy is occurring, but it is theoretically possible that an additional single-membrane process involving LC3-II, ATG5, and beclin1, such as LC3-associated phagocytosis (LAP) (Martinez et al., 2011; Florey et al., 2011), is also operational. Moreover, whether the effects on apoptosis, oxidative stress, and efferocytosis involve classic macroautophagy or, for example, chaperone-mediated autophagy or mitophagy, remains to be established. While our data implicate the role of NADPH oxidase, they do not role out other sources of oxidative stress, such as mitochondria, which could be affected by mitophagy (Scherz-Shouval and Elazar, 2011). Second, how the factors studied here, and those that actually function in atherosclerotic lesions, induce autophagy is not known. While ER stress has been reported to induce autophagy (Kroemer et al., 2010), we found that silencing key molecules in the IRE1 and PERK branches of the UPR did not block autophagy initiation or flux through lysosomes (data not shown). Third, the mechanism involved in defective efferocytosis of autophagy-inhibited apoptotic macrophages requires further study. The data here indicate that autophagosomal flux through lysosomes in cells undergoing apoptosis somehow increases their recognition by phagocytes, perhaps by increasing the expression of a cell-surface recognition molecule. However, we found no evidence of a defect in PS externalization or presentation of three other efferocytosis ligands, calreticulin, ERp57, and pentraxin 3, in autophagy-inhibited macrophages (data not shown).

Future studies will likely reveal additional roles of autophagy in atherosclerosis that are cell type- and lesion stage-specific. For example, previous work has shown that intimal smooth muscle cells can acquire morphological features suggestive of autophagy (De Meyer and Martinet, 2009), although the functional significance of this finding is unknown. Links between autophagy and inflammation have been implicated in other disease models (Levine et al., 2011), which could be important in atherosclerosis if such processes occurred in lesional cells. A recent study revealed that autophagy can play a role in the hydrolysis of stored cholesteryl ester droplets in macrophages, thus facilitating cholesterol efflux (Ouimet

et al., 2011), but the relevance of this finding to atherosclerosis remains to be determined. Knowledge gained from autophagy studies in atherosclerosis may be useful for devising mechanism-based therapeutic strategies. Although increasing autophagy above the induced level with rapamycin or ATG7 transduction did not protect macrophage *in vitro*, autophagy appears to be defective in advanced atherosclerosis, and so restoring autophagy to the normally induced level may be protective. Moreover, boosting autophagy did improve efferocytosis *in vitro*, which may translate into a beneficial effect in advanced atherosclerosis (Tabas, 2010). Such strategies would be unique, because autophagy may be the macrophage's natural way to combat two complementary processes in plaque necrosis, macrophage apoptosis and defective efferocytosis.

EXPERIMENTAL PROCEDURES

Animals and Diets

C57BL/6J, *Ldlr* $^{-/-}$, *Nox2* $^{-/-}$, and *ob/ob* mice were purchases from Jackson Laboratory (Bar Harbor, Maine). The GFP-LC3 transgenic and *Atg5*$^{fl/fl}$ mice (Mizushima and Kuma, 2008; Hara et al., 2006) were created by Dr. Noboru Mizushima, Tokyo Medical and Dental University, and sent to us from the laboratory of Dr. Beth Levine (University of Texas, Southwestern). The *Lysmcre*$^{+/-}$ mice (Clausen et al., 1999) were from Dr. Irmgard Föster (Technical University of Munich). The *Ldlr*$^{-/-}$, *Atg5*$^{fl/fl}$, and *Lysmcre* mice were bred with each other to generate the mice used for this study. For the atherosclerosis study, 8-wk-old female mice were placed on a Western-type diet (TD88137; Harlan Teklad) for the indicated number of weeks.

Apoptosis Assays

Apoptosis was assayed in cultured macrophages by staining with Alexa 488-conjugated Annexin V or using the TUNEL (TdT-mediated dUTP nick-end labeling) protocol, as described previously (Seimon et al., 2010). Apoptotic cells in atherosclerotic lesions were labeled by TUNEL using the *in situ* cell death detection kit TMR-red (Roche Diagnostics) according to the manufacturer's protocol. Only TUNEL-positive cells that co-localized with DAPI-stained nuclei were counted as being positive. Lesional apoptosis was also assayed by immunofluorescence using anti-activated caspase-3 primary antibody. TUNEL, annexin V, and activated caspase-3 staining were viewed using an Olympus IX-70 inverted fluorescent microscope. Representative fields (4–6 fields containing ~2000 cells) were photographed using an Olympus DP71 CCD camera. The number of Annexin V-positive cells were counted and expressed as a percent of the total number of cells in at least 4 separate fields from duplicate wells. For TUNEL analysis of lesions, DAPI and TUNEL images were merged using Photoshop analysis software (Adobe Systems). The number of cells positive for TUNEL or activated caspase-3 was quantified as a percentage of total lesional cells in macrophage-rich regions.

Atherosclerotic Lesion Analysis

For morphometric lesion analysis, sections were stained with Harris' hematoxylin and eosin. The total lesion area and necrotic area were quantified as previously described (Seimon et al., 2009). For plaque necrosis, boundary lines were drawn around regions that were free of H&E staining, and area measurements were obtained using image analysis software. A 3,000-μm^2 threshold was implemented in order to avoid counting regions that likely do not represent substantial areas of necrosis. Using this method, a 97% agreement in the percent necrotic area was calculated between our 2 independent observers. The methods for DHE and $p47^{phox}$ staining appear in Supplemental Experimental Procedures.

Statistics

Values are given as means ± S.E.M. (n = 4 unless otherwise noted in the figure legends); absent error bars in the bar graphs signify S.E.M. values smaller than the graphic symbols. Comparison of mean values between groups was evaluated using a two-tailed student t-test, Mann-Whitney U test, or ANOVA. P values less than 0.05 was considered significant. Refer to the legend of Figure S3C for additional statistical methods specific for the analysis of the data in that panel.

Supplementary Material

Refer to Web version on PubMed Central for supplementary material.

Acknowledgments

This work was supported by NIH grants HL106019, HL075662, and HL054591 (I.T.) and by fellowships of the Netherlands Organization of Scientific research (Rubicon) and the international atherosclerosis society (J.C.S.). The authors acknowledge Dr. Noboru Mizushima and his institution, Tokyo Medical and Dental University, for allowing the use of *Atg5*$^{fl/fl}$ mice and GFP-LC3 transgenic mice for these studies. The authors thank Dr. Edward Thorp and George Kuriakose, Columbia University, for helpful advice on the efferocytosis experiments and for technical support, respectively; Dr. Beth Levine, University of Texas, Southwestern, for her advice and support during the course of this project; Dr. Douglas R. Green, St. Jude Children's Research Hospital, for helpful discussions; Dr. Marlys Koschinsky, University of Windsor, Ontario, for providing the recombinant apo(a); and Drs. Rajasekhar Ramakrishnan and Steve Holleran for help with statistical analysis.

References

Ball RY, Stowers EC, Burton JH, Cary NR, Skepper JN, Mitchinson MJ. Evidence that the death of macrophage foam cells contributes to the lipid core of atheroma. Atherosclerosis. 1995; 114:45–54. [PubMed: 7605375]

Bjorkoy G, Lamark T, Pankiv S, Overvatn A, Brech A, Johansen T. Monitoring autophagic degradation of p62/SQSTM1. Methods Enzymol. 2009; 452:181–197. [PubMed: 19200883]

Clarke R, Peden JF, Hopewell JC, Kyriakou T, Goel A, Heath SC, Parish S, Barlera S, Franzosi MG, Rust S, Bennett D, Silveira A, Malarstig A, Green FR, Lathrop M, Gigante B, Leander K, de FU, Seedorf U, Hamsten A, Collins R, Watkins H, Farrall M. Genetic variants associated with Lp(a) lipoprotein level and coronary disease. N Engl J Med. 2009; 361:2518–2528. [PubMed: 20032323]

Clausen BE, Burkhardt C, Reith W, Renkawitz R, Forster I. Conditional gene targeting in macrophages and granulocytes using LysMcre mice. Transgenic Res. 1999; 8:265–277. [PubMed: 10621974]

De Meyer GR, Martinet W. Autophagy in the cardiovascular system. Biochim Biophys Acta. 2009; 1793:1485–1495. [PubMed: 19152812]

Eisenberg-Lerner A, Bialik S, Simon HU, Kimchi A. Life and death partners: apoptosis, autophagy and the cross-talk between them. Cell Death Differ. 2009; 16:966–975. [PubMed: 19325568]

Feng B, Yao PM, Li Y, Devlin CM, Zhang D, Harding HP, Sweeney M, Rong JX, Kuriakose G, Fisher EA, Marks AR, Ron D, Tabas I. The endoplasmic reticulum is the site of cholesterol-induced cytotoxicity in macrophages. Nat Cell Biol. 2003a; 5:781–792. [PubMed: 12907943]

Feng B, Zhang D, Kuriakose G, Devlin CM, Kockx M, Tabas I. Niemann-Pick C heterozygosity confers resistance to lesional necrosis and macrophage apoptosis in murine atherosclerosis. Proc Natl Acad Sci U S A. 2003b; 100:10423–10428. [PubMed: 12923293]

Florey O, Kim SE, Sandoval CP, Haynes CM, Overholtzer M. Autophagy machinery mediates macroendocytic processing and entotic cell death by targeting single membranes. Nat Cell Biol. 2011; 13:1335–1343. [PubMed: 22002674]

Hara T, Nakamura K, Matsui M, Yamamoto A, Nakahara Y, Suzuki-Migishima R, Yokoyama M, Mishima K, Saito I, Okano H, Mizushima N. Suppression of basal autophagy in neural cells causes neurodegenerative disease in mice. Nature. 2006; 441:885–889. [PubMed: 16625204]

Henson PM, Bratton DL, Fadok VA. Apoptotic cell removal. Curr Biol. 2001; 11:R795–R805. [PubMed: 11591341]

Huang J, Canadien V, Lam GY, Steinberg BE, Dinauer MC, Magalhaes MA, Glogauer M, Grinstein S, Brumell JH. Activation of antibacterial autophagy by NADPH oxidases. Proc Natl Acad Sci U S A. 2009; 106:6226–6231. [PubMed: 19339495]

Kroemer G, Marino G, Levine B. Autophagy and the integrated stress response. Mol Cell. 2010; 40:280–293. [PubMed: 20965422]

Levine B, Mizushima N, Virgin HW. Autophagy in immunity and inflammation. Nature. 2011; 469:323–335. [PubMed: 21248839]

Li G, Mongillo M, Chin KT, Harding H, Ron D, Marks AR, Tabas I. Role of ERO1α-mediated stimulation of inositol 1, 4, 5-triphosphate receptor activity in endoplasmic reticulum stress-induced apoptosis. J Cell Biol. 2009; 186:783–792. [PubMed: 19752026]

Li G, Scull C, Ozcan L, Tabas I. NADPH oxidase links endoplasmic reticulum stress, oxidative stress, and PKR activation to induce apoptosis. J Cell Biol. 2010; 191:1113–1125. [PubMed: 21135141]

Lizard G, Gueldry S, Sordet O, Monier S, Athias A, Miguet C, Bessede G, Lemaire S, Solary E, Gambert P. Glutathione is implied in the control of 7-ketocholesterol-induced apoptosis, which is associated with radical oxygen species production. FASEB J. 1998; 12:1651–1663. [PubMed: 9837855]

Lusis AJ. Atherosclerosis. Nature. 2000; 407:233–241. [PubMed: 11001066]

Martinez J, Almendinger J, berst AS, ess R, Dillon CP, Fitzgerald P, Hengartner MO, Green DR. Microtubule-associated protein 1 light chain 3 alpha (LC3)-associated phagocytosis is required for the efficient clearance of dead cells. Proc Natl Acad Sci U S A. 2011 In Press.

Mizushima N, Kuma A. Autophagosomes in GFP-LC3 Transgenic Mice. Methods Mol Biol. 2008; 445:119–124. [PubMed: 18425446]

Mizushima N, Yoshimori T, Levine B. Methods in mammalian autophagy research. Cell. 2010; 140:313–326. [PubMed: 20144757]

Moore KJ, Tabas I. Macrophages in the pathogenesis of atherosclerosis. Cell. 2011; 145:341–355. [PubMed: 21529710]

Myoishi M, Hao H, Minamino T, Watanabe K, Nishihira K, Hatakeyama K, Asada Y, Okada K, Ishibashi-Ueda H, Gabbiani G, Bochaton-Piallat ML, Mochizuki N, Kitakaze M. Increased endoplasmic reticulum stress in atherosclerotic plaques associated with acute coronary syndrome. Circulation. 2007; 116:1226–1233. [PubMed: 17709641]

Ouimet M, Franklin V, Mak E, Liao X, Tabas I, Marcel YL. Autophagy regulates cholesterol efflux from macrophage foam cells via lysosomal acid lipase. Cell Metab. 2011; 13:655–667. [PubMed: 21641547]

Pattison JS, Osinska H, Robbins J. Atg7 induces basal autophagy and rescues autophagic deficiency in CryABR120G cardiomyocytes. Circ Res. 2011; 109:151–160. [PubMed: 21617129]

Qu X, Zou Z, Sun Q, Luby-Phelps K, Cheng P, Hogan RN, Gilpin C, Levine B. Autophagy gene-dependent clearance of apoptotic cells during embryonic development. Cell. 2007; 128:931–946. [PubMed: 17350577]

Scherz-Shouval R, Elazar Z. Regulation of autophagy by ROS: physiology and pathology. Trends Biochem Sci. 2011; 36:30–38. [PubMed: 20728362]

Schrijvers DM, De Meyer GR, Kockx MM, Herman AG, Martinet W. Phagocytosis of apoptotic cells by macrophages is impaired in atherosclerosis. Arterioscler Thromb Vasc Biol. 2005; 25:1256–1261. [PubMed: 15831805]

Seimon TA, Liao X, Magallon J, Moore KJ, Witztum JL, Tsimikas S, Golenbock DT, Webb NR, Tabas I. Atherogenic lipids and lipoproteins trigger CD36-TLR2-dependent apoptosis in macrophages undergoing endoplasmic reticulum stress. Cell Metabolism. 2010; 12:467–482. [PubMed: 21035758]

Seimon TA, Wang Y, Han S, Senokuchi T, Schrijvers DM, Kuriakose G, Tall AR, Tabas IA. Macrophage deficiency of p38alpha MAPK promotes apoptosis and plaque necrosis in advanced atherosclerotic lesions in mice. J Clin Invest. 2009; 119:886–898. [PubMed: 19287091]

Tabas I. Macrophage death and defective inflammation resolution in atherosclerosis. Nature Rev Immunol. 2010; 10:36–46. [PubMed: 19960040]

Thorp E, Cui D, Schrijvers DM, Kuriakose G, Tabas I. Mertk receptor mutation reduces efferocytosis efficiency and promotes apoptotic cell accumulation and plaque necrosis in atherosclerotic lesions of *Apoe*−/− mice. Arterioscler Thromb Vasc Biol. 2008; 28:1421–1428. [PubMed: 18451332]

Virmani R, Burke AP, Kolodgie FD, Farb A. Vulnerable plaque: the pathology of unstable coronary lesions. J Interv Cardiol. 2002; 15:439–446. [PubMed: 12476646]

HIGHLIGHTS

- Pro-apoptotic oxidative stress induces autophagy in macrophages (Mφs)
- Inhibition of autophagy enhances oxidative stress and apoptosis in Mφs
- Atheromata of Mφ-*Atg5*$^{-/-}$*Ldlr*$^{-/-}$ mice have increased apoptosis and plaque necrosis
- Apoptotic *Atg5*$^{-/-}$ Mφs are poorly recognized by phagocytes *in vitro* and in atheromata

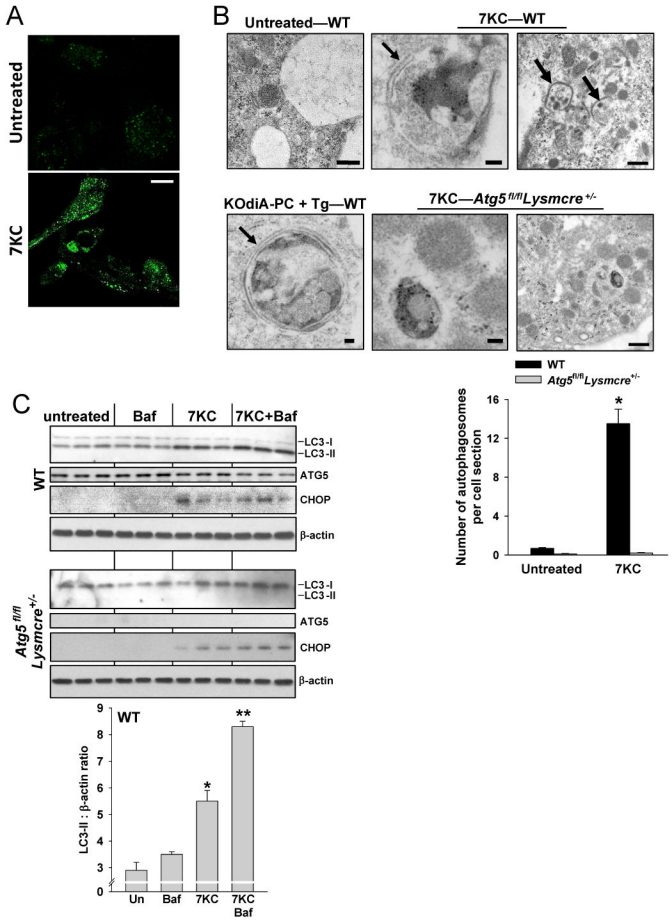

Figure 1. Autophagy is Induced in Macrophages Exposed to Atherosclerosis-Related Stimulators of Apoptosis

(A) Confocal fluorescence microscopy of macrophages from GFP-LC3 transgenic mice that were left untreated or treated for 8 h with 35 μM 7-ketocholesterol (7KC). Bar = 10 μm.

(B) Electron microscopy of macrophages from WT or *Atg5*$^{fl/fl}$*LysmCre*$^{+/-}$ mice that were left untreated or treated for 6 h with 7KC or 50 μg/ml of KOdiA-PC plus 0.5 μM thapsigargin (KOdiA-PC + Tg). Double-membranes are depicted by arrows. Bar, 100 nm for left and middle row of images and 500 nm for right row of images. Quantification of the average number of autophagosomes per cell section in untreated and 7KC-treated WT and *Atg5*$^{fl/fl}$*LysmCre*$^{+/-}$ macrophages is shown (mean ± S.E.M.; *p < 0.01 vs. other groups; n = 10 cell sections/group).

(C) Macrophages from WT or *Atg5*$^{fl/fl}$*LysmCre*$^{+/-}$ mice were left untreated or incubated for 4 h with 7KC. In some groups, 10 μM bafilomycin A1 (Baf) was added during the last 2 h. Cell extracts were probed for LC3-I, LC3-II, Atg5, CHOP, and β-actin by immunoblot. Densitometric quantification of the WT immunoblot data are shown in the graph (mean ± S.E.M.; *,**p < 0.05 vs. the other groups and each other).

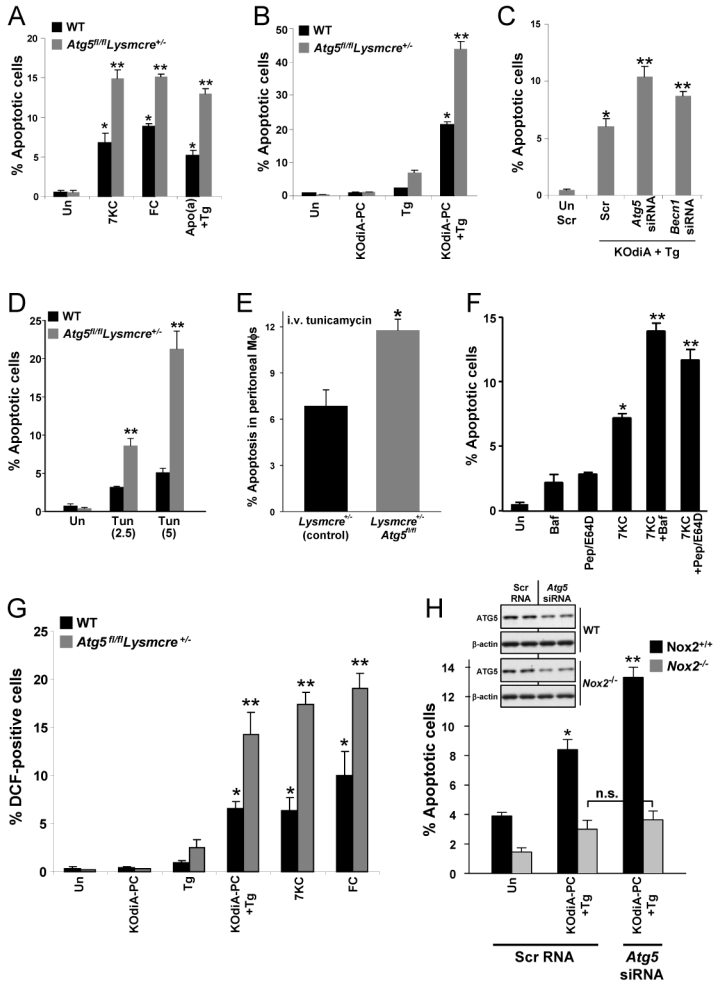

Figure 2. Inhibition of Autophagy Increases Apoptosis and NADPH Oxidase-Mediated Oxidative Stress

For (A) – (D), macrophages from WT or *Atg5*$^{fl/fl}$*LysmCre*$^{+/-}$ mice were left untreated (Un) or incubated as below and then assayed for apoptosis by annexin V staining (mean ± S.E.M.; *p < 0.05, **p < 0.01 vs. the other groups).

(A) Incubation times were 20 h for 7KC, 18 h for free cholesterol (FC)-loading, and 20 h for 50 μg/ml apolipoprotein(a) [Apo(a)] plus 0.5 μM thapsigargin (Tg).

(B) Incubation time was 24 h for 50 μg/ml of KOdiA-PC alone, 0.5 μM thapsigargin (Tg) alone, or both reagents together.

(C) As in (B), but the cells were pre-treated for 90 h with either scrambled RNA (Scr) or siRNA targeting *Atg5* or *Becn1*.

(D) Incubation times were 24 h for 2.5 or 5.0 μg/ml tunicamycin (Tun).

(E) *Lysmcre*$^{+/-}$ (control) and *Atg5*$^{fl/fl}$*Lysmcre*$^{+/-}$ mice were injected i.v. with 0.02 mg/kg tunicamycin, and 16 h later freshly harvested peritoneal macrophages were assayed for apoptosis using annexin V (mean ± S.E.M.; *p < 0.05).

(F) Incubation time was 20 h for 7KC in the absence or presence of either 20 nM bafilomycin A1 or 10 μg/ml of pepstatin plus 10 μg/ml of E64D.

(G) Macrophages from WT or *Atg5*$^{fl/fl}$*Lysmcre*$^{+/-}$ mice were left untreated or incubated with the indicated reagents as above. The cells were then stained with DCFDA, viewed by fluorescence microscopy, and quantified for the percent of DCF-positive cells (mean ± S.E.M.; *p < 0.05, **p < 0.01 vs. the other groups).

(H) Macrophages from *Nox2*$^{+/+}$ or *Nox2*$^{-/-}$ mice were left untreated or incubated with KOdiA-PC plus thapsigargin and then assayed for apoptosis, except some of the cells were pre-treated for 90 h with scrambled RNA or *Atg5* siRNA. The inset shows the immunoblot of ATG5 and β-actin in macrophages treated with scrambled RNA or *Atg5* siRNA (mean ± S.E.M.; *$p < 0.05$, **$p < 0.01$ vs. the other groups; n.s. = not significant).

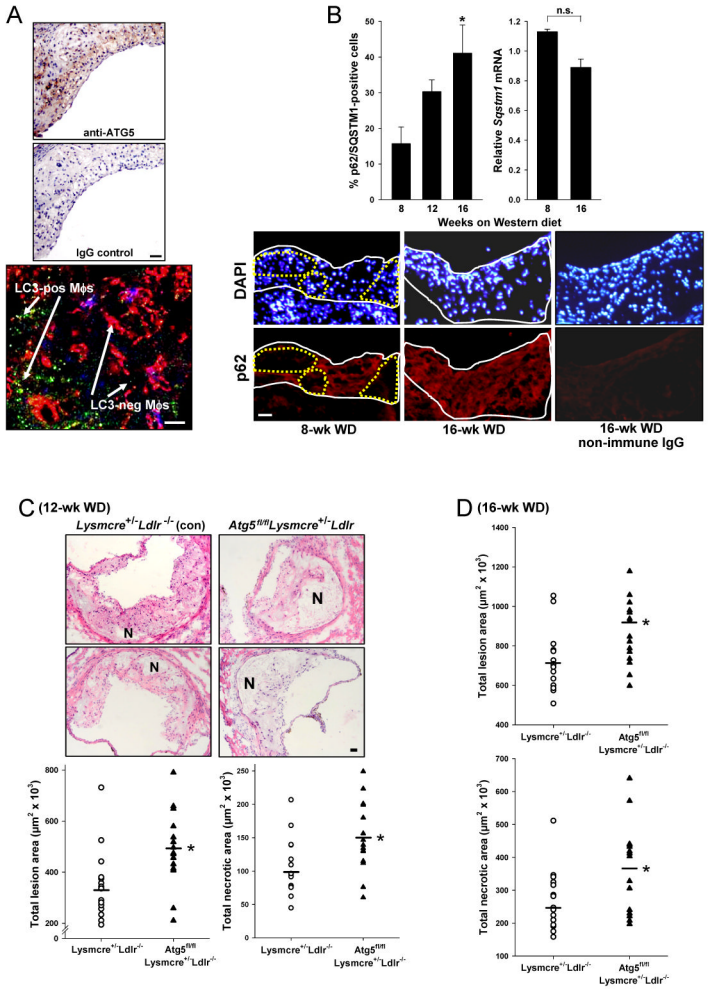

Figure 3. Defective Macrophage Autophagy Promotes Plaque Necrosis in Advanced Atherosclerotic Lesions of Western diet (WD)-Fed *Ldlr*$^{-/-}$ Mice

(A) Female GFP-LC3-*Ldlr*$^{-/-}$ mice were fed the WD for 12 wks. Cross-sections of an aortic root lesion were immunostained with anti-ATG5 or control IgG (top images; bar = 20 μm) or with anti-F4/80 antibody and viewed by confocal fluorescence microscopy (bottom image; red = F4/80, green = GFP-LC3; bar = 10 μm).

(B) Female *Lysmcre*$^{+/-}$*Ldlr*$^{-/-}$ (control) and *Atg5*$^{fl/fl}$*Lysmcre*$^{+/-}$*Ldlr*$^{-/-}$ mice were fed the WD for 8, 12, or 16 wks (n = 5 per group). Lesions were then immunostained for p62/SQSTM1 and DAPI (nuclei), and lesional *Sqstm1* mRNA was assayed by LCM-RT-qPCR (mean ± S.E.M.; *p = 0.02 vs. 8-wk value; n.s., not significant). Representative images for the p62 immunostaining data are shown for the 8- and 16-wk lesions, along with a non-immune control image for a 16-wk lesion. Bar, 20 μm. In these images, the intima, which is composed mostly of macrophages, is outlined by the solid white lines, and areas of the 8-wk intima that have cells negative for p62 are outlined by the dotted yellow line.

(C–D) Aortic root sections of female *Lysmcre*$^{+/-}$*Ldlr*$^{-/-}$ (control) and *Atg5*$^{fl/fl}$*Lysmcre*$^{+/-}$*Ldlr*$^{-/-}$ mice fed the WD for 12 or 16 wks were stained with H&E and then quantified for lesion and necrotic area. Representative images are shown for the 12-wk groups. N, necrotic area; Bar, 20 μm (mean ± S.E.M.; *p < 0.05; n con/experimental = 15/15 for the 12-wk cohort and 17/15 for the 16-wk cohort).

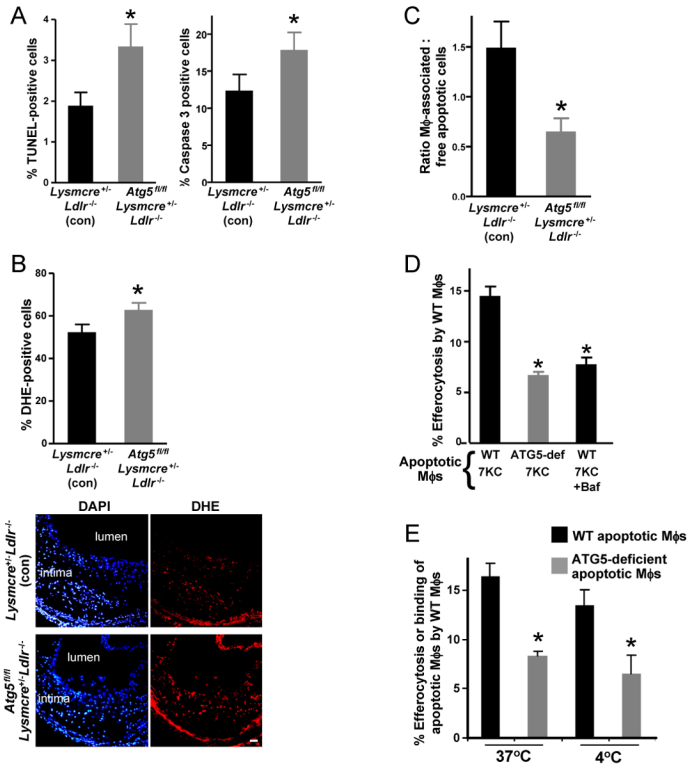

Figure 4. Defective Macrophage Autophagy Promotes Apoptosis, Oxidative Stress, and Defective Efferocytosis

(A–B) Sections from the 12-wk cohort in Fig.3 were stained for TUNEL, activated caspase-3, or DHE and then counterstained with DAPI (nuclei) and quantified (mean ± S.E.M.; *p < 0.05; n = 15 con/15 experimental). Bar = 20 μm.

(C) The lesions were stained for TUNEL and for F4/80 (macrophages), and the ratio of TUNEL-positive cells that were F4/80-associated or not (“free”) was quantified (mean ± S.E.M.; *p < 0.05; n = 15 con/15 experimental).

(D) Macrophages from WT or *Atg5*$^{fl/fl}$*LysmCre*$^{+/-}$ mice were rendered apoptotic using 7KC; one set of WT cells was also treated with bafilomycin A1 (Baf). These cells were then added to WT macrophages, and efferocytosis was assayed and expressed as the percent of WT macrophages with ingested apoptotic cells (mean ± S.E.M.; *p < 0.01).

(E) The experiment labeled “37°C” was similar to the 1st and 2nd experimental groups in panel D. The experiment labeled “4°C” assayed the binding of WT and *Atg5*$^{fl/fl}$*LysmCre*$^{+/-}$ apoptotic macrophages to WT macrophages (mean ± S.E.M.; *p < 0.01).